Damage and thermal annealing of dual-ions (Pt and S) implanted ⟨100⟩ YSZ material

1997 J. Phys.: Condens. Matter 9 4377

(http://iopscience.iop.org/0953-8984/9/21/005)

J. Phys.: Condens. Matter **9** (1997) 4377–4383. Printed in the UK PII: S0953-8984(97)80993-9

Damage and thermal annealing of dual-ions (Pt and S) implanted ⟨100⟩ YSZ material

Dong-zhu Xie, De-zhang Zhu and De-xin Cao

Laboratory of Nuclear Analysis Techniques, Shanghai Institute of Nuclear Research, Academia Sinica, Shanghai 201800, People's Republic of China

Received 15 January 1997, in final form 18 March 1997

Abstract. A ⟨100⟩ oriented cubic YSZ (yttria stabilized zirconia) single crystal implanted with 160 keV platinum ions and subsequently implanted with 40 keV sulphur ions has been investigated. The implantation was carried out at room temperature (RT). Annealing was performed isothermally in air ambient at 850 °C and 1100 °C for 4 and 12 hours. Rutherford backscattering spectrometry and channelling (RBS-C) of 2 MeV He ions was used to study the depth distribution of lattice damage and impurity, as well as the recrystallization of the damaged layer. X-ray diffraction (XRD) is employed to examine the phase formation. For dual-implanted samples, XRD measurement showed, after annealing, formation of monoclinic phase polycrystalline ZrO_2 in the damage region and Pt grains with randomly oriented cubic phase, which is consistent with RBS-C results. In addition, XRD measurement also revealed formation of hexagonal PtS_2 grains.

1. Introduction

Ytrria stabilized zirconia (YSZ) ceramics are well known as oxide ion conductors. They are used in applications like oxygen sensors, oxygen pumps, fuel cells [1], humidity sensors [2] and used as buffer layers for high-temperature superconducting thin film growth with promising results [3–5]. For the applications as an oxygen ion conductor, it is necessary to put an electronically conducting electrode material on top of the YSZ matrix. Conventionally this electrode material is Pt [6, 7] because of its good catalysis for decomposition of oxygen gas molecules. The top Pt thin-film layer can be obtained by several methods, e.g. ion beam assisted deposition [8] and chemical vapour deposition [9, 10]. In many applications paste Pt electrodes are used too [11, 12]. But top layers formed by implantation have the advantages that they can be made thin and that no sharp interface exists between the top layer and the YSZ matrixes. Furthermore nonequilibrium compositions and microstructures can be realized. As an oxygen ion conductor, it is often used in an ambient which contains sulphur gas, e.g. in a monitor of car tail gas. The interactions between sulphur and platinum and ZrO_2 may be one of factors that affect the lifetime of oxygen sensors. So far, there is no report about the effect of sulphur on YSZ material to our knowledge. As a part of a series of investigations of YSZ material, this paper is concerned with reporting the microstructure of YSZ implanted with platinum and subsequently sulphur followed by isothermal annealing. The effects of sulphur on oxygen decomposition and pumping between the gas and Pt electrode and YSZ electrolyte are under investigation.

0953-8984/97/214377+07$19.50

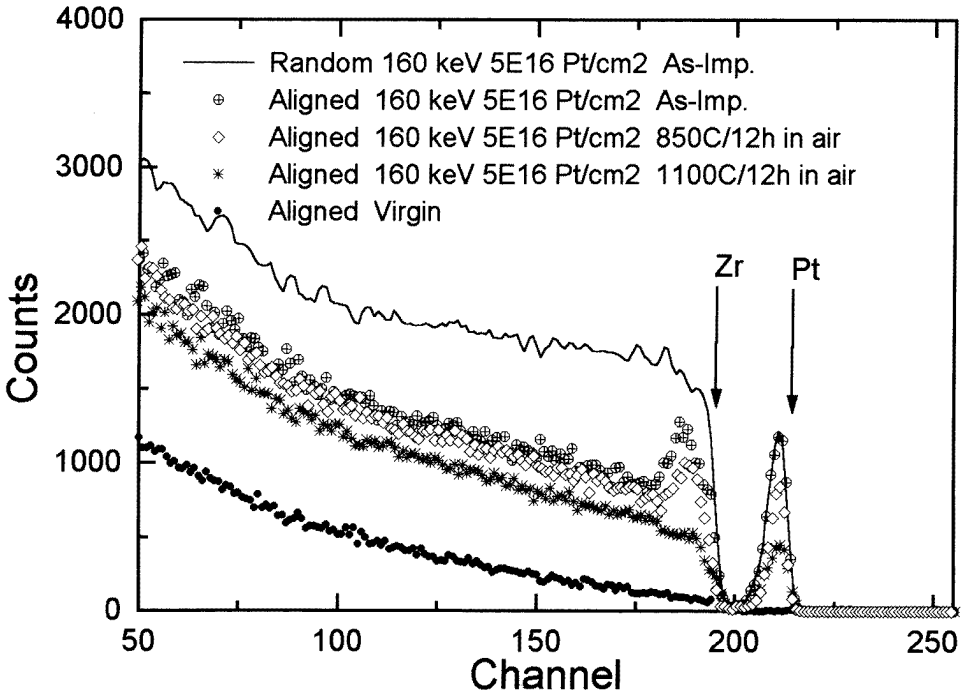

Figure 1. 2 MeV He^+ RBS-C spectra of 160 keV 5×10^{16} Pt cm^{-2} implanted sample before and after annealing at the indicated temperatures for 12 hours (the scattering angle is 165°, energy calibration is: $\epsilon = 8.41$ keV/channel and $E_0 = 41.33$ keV, E_0 is the offset of the MCA).

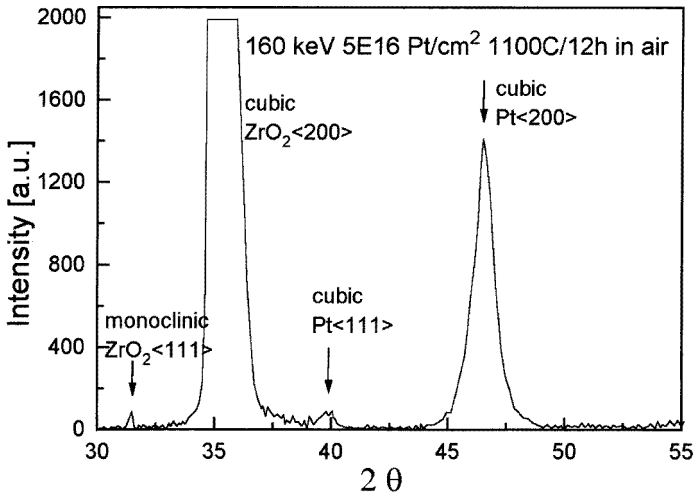

Figure 2. XRD pattern of sample implanted with 5×10^{16} Pt cm^{-2} after annealing at 1100 °C for 12 hours: besides Pt ⟨200⟩ peak the Pt ⟨111⟩ peak was also observed.

2. Experimental details

The ZrO_2 ⟨100⟩ single crystal used in this investigation (obtained from Ceres Corporation, USA) was doped with 9.5 mol% yttria in order to stabilize the cubic phase. Platinum

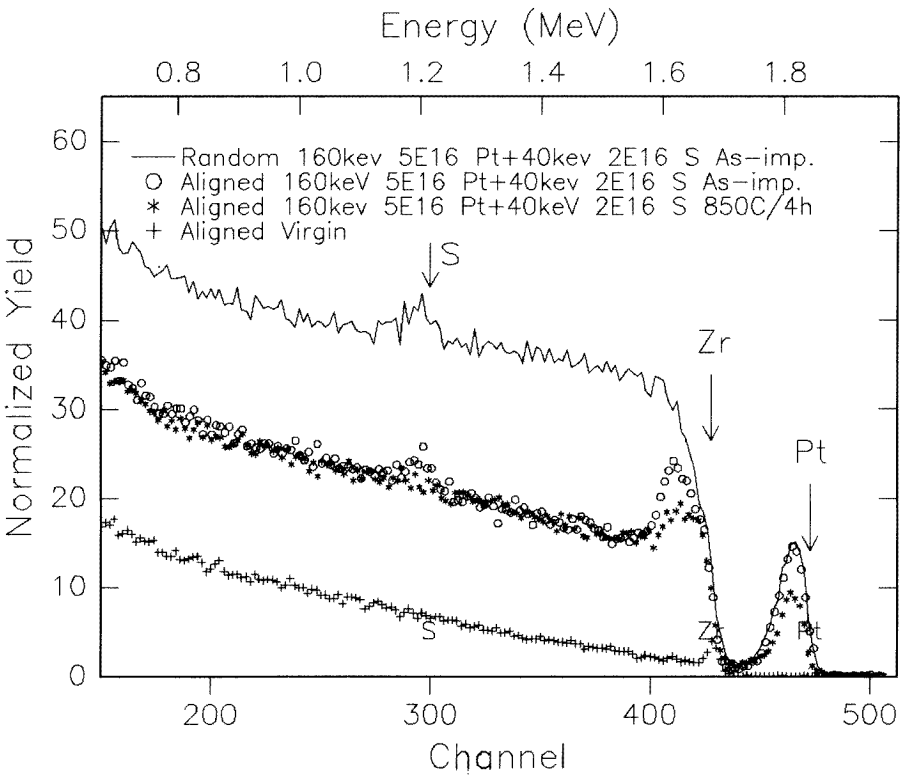

Figure 3. RBS-C spectra of 160 keV 5×10^{16} Pt cm^{-2} and 40 keV 2×10^{16} S cm^{-2} implanted sample before and after annealing at 850 °C for 4 hours (the scattering angle is 170 °, energy calibration is: $\epsilon = 3.63$ keV/channel and $E_0 = 129.0$ keV).

implantation was carried out at room temperature (RT) using a metal vapour vacuum arc (MEVVA) high-current ion implanter at Beijing Normal University. The MEVVA source produces ions with multiple charge states leading to effectively multi-energy implants. For our experiment the average charge state of Pt was 2.1 (Pt^{1+}, 11%; Pt^{2+}, 70%; Pt^{3+}, 18%; Pt^{4+}, 1%) corresponding to an average energy of 160 keV for Pt ions extracted at 76 kV. A nominal dose of 5×10^{16} ions cm^{-2} was used. Sulphur implantation was performed at room temperature using an isotopic separator at Shanghai Institute of Nuclear Research. 40 keV energy and doses of 2×10^{16} ions cm^{-2} and 5×10^{16} ions cm^{-2} were used; the beam current density is less than 2 μA cm^{-2} to keep the specimen at RT as far as possible. Annealing of the implanted samples was performed in air ambient at 850 °C and 1100 °C for 4 and 12 hours.

Rutherford backscattering spectrometry and channelling (RBS-C) of 2 MeV He ions was used to study the depth distribution of lattice damage and impurity, as well as the recrystallization of the damaged layer. X-ray diffraction (XRD) with Cu Kα radiation was used to examine the crystallite phase of implanted platinum and the recrystallization of the damaged region of YSZ.

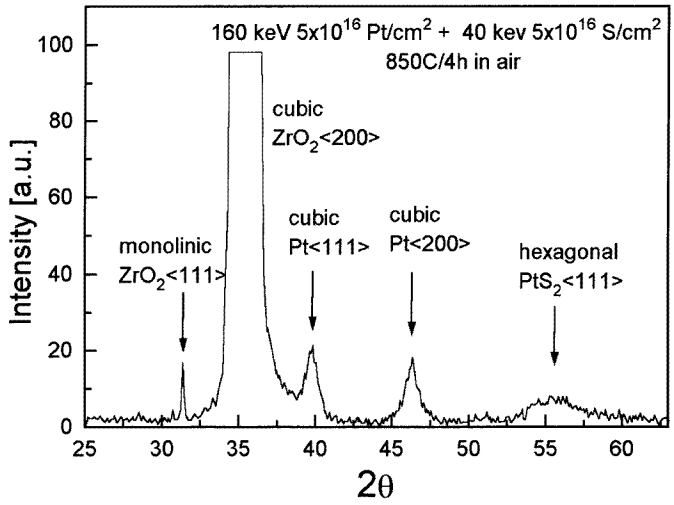

Figure 4. XRD pattern of sample implanted with 5×10^{16} Pt cm^{-2} and 40 keV 5×10^{16} S cm^{-2} after annealing at 850 °C for 4 hours: besides the Pt ⟨200⟩ peak, the Pt ⟨111⟩, Pt ⟨220⟩, Pt ⟨222⟩, monoclinic ZrO_2 ⟨111⟩, ⟨222⟩ and hexagonal PtS_2 ⟨111⟩ peaks were also observed.

3. Results and discussion

Figure 1 shows the random and aligned backscattering spectra of a sample singly implanted with 160 keV Pt to a nominal dose of 5×10^{16} ions cm^{-2}. It can been seen from figure 1 that Pt ion implantation creates heavy damage in the sub-surface region, but not amorphization, and the outermost surface was relatively slightly damaged. From the random spectrum of the as-implanted sample the number of Pt ions was calculated to be 2.94×10^{16} ions cm^2. The difference between the nominal dose and the calculated dose may arise from: (a) accuracy of dose measurement in MEVVA source because of no charge selection as well as the nonuniform cross section density of the large-area beam current and (b) sputtering effect. The peak of platinum ion distribution was located at a depth of about 32 nm from the surface, which is calculated from the Pt spectrum (shown in figure 1). The radiation damage peak with its maximum of $\chi(\mathrm{Zr}) = 0.75$ was located at a depth of about 64 nm from the surface (χ is defined in the usual way as the ratio of the aligned to random yield). The depth of the damage peak is much larger than the projected range (32 nm) of 160 keV platinum ions in ZrO_2. This result could be interpreted in terms of high-dose implantation and self-annealing effect of room-temperature implantation. The damage is initially increased as increasing implanted dose, then reaches saturation but not amorphization at the damage peak because of self-annealing. Further increasing of the implanted dose causes the damage peak to become wider. Consequently, for implantation of high-dose Pt in YSZ material the depth of the damage peak is larger than the projected range of Pt ions. Similar results were observed for YSZ implanted with 105 keV 2×10^{16} Pt cm^{-2} at RT [13] and for sapphire implanted with indium at RT [14].

Figure 1 also shows the RBS-C spectra after annealing at 850 °C and 1100 °C for 12 hours, which indicate that the interface of substrate and damage layer moves towards the surface during thermal annealing, and the height of the damage peak is reduced concurrently. Consequently, it is quite different from conventional solid phase epitaxy. It also can be seen from figure 1 that the outermost surface is recrystallized well after 12 hours annealing. XRD

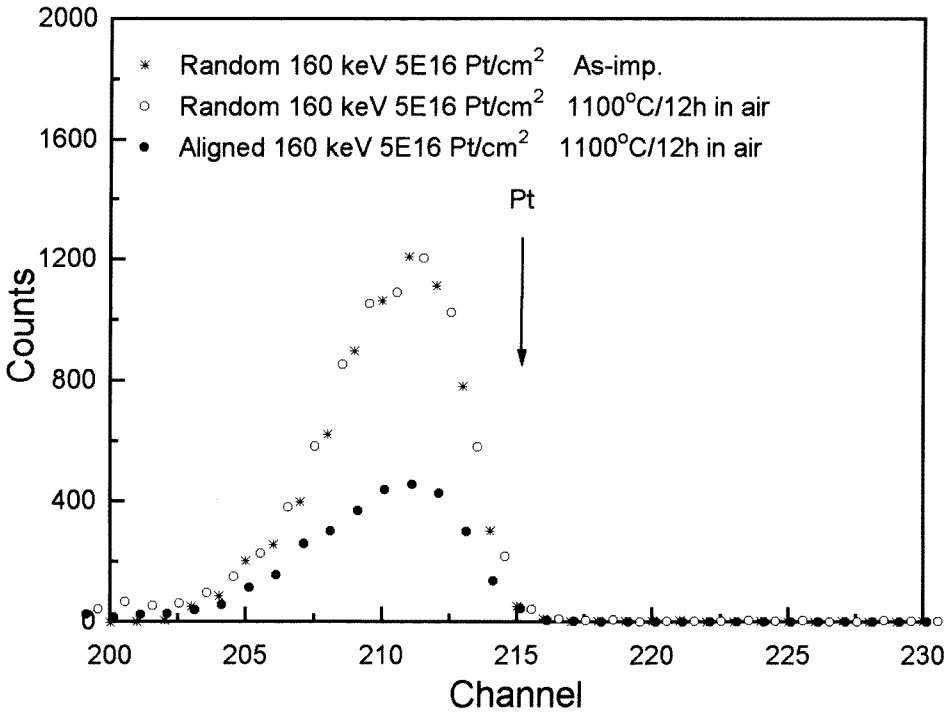

Figure 5. Annealing behaviours of platinum depth profiles for 160 keV 5×10^{16} Pt cm^{-2} implanted sample at 1100 °C for 12 hours (the scattering angle is 165°, energy calibration is: $\epsilon = 8.41$ keV/channel and $E_0 = 41.33$ keV).

measurement (shown in figure 2) indicates that a small fraction of monoclinic ZrO_2 has been formed in the damage region.

For platinum and sulphur dual-implanted samples the RBS-C spectra, before and after annealing at 850 °C for 4 hours, are shown in figure 3. The projected ranges calculated by TRIM-92 are about 32 nm for 160 keV Pt ions (mean energy of Pt ions; the mean projected range of an ensemble of ions of 11% Pt^{1+}, 70% Pt^{2+}, 18% Pt^{3+}, 1% Pt^{4+} is 31.6 nm calculated by TRIM-92) and 28 nm for 40 keV S ions. So the Pt and S ions are essentially located in the same region. The symbol χ(Zr) at the damage peak was calculated from the as-implanted spectrum in figure 3 to be about 0.75. Comparison of the as-implanted spectrum in figure 3 with that in figure 1 shows that for dual implantation the damage region becomes wider; the outermost surface was damaged heavily, while χ(Zr) at the damage peak was still about 0.75. After annealing the residual damage in the outermost surface region is still heavy. Figure 4 shows the XRD results of a sample implanted with 160 keV 5×10^{16} Pt cm^{-2} and 40 keV 5×10^{16} S cm^{-2} after annealing at 850 °C for 4 hours. It can be seen from figure 4 that monoclinic phase ZrO_2 crystallites have been formed and the ⟨111⟩ orientation diffraction peak is much higher than that of the singly implanted sample (shown in figure 2), which reveals that there is an intensive interaction between sulphur and YSZ material.

There is a large difference of platinum annealing behaviour between the singly implanted and dual-implanted samples. Figure 5 shows the annealing results of 160 keV 5×10^{16} Pt ions cm^{-2} singly implanted samples. There is no loss of Pt ions even after

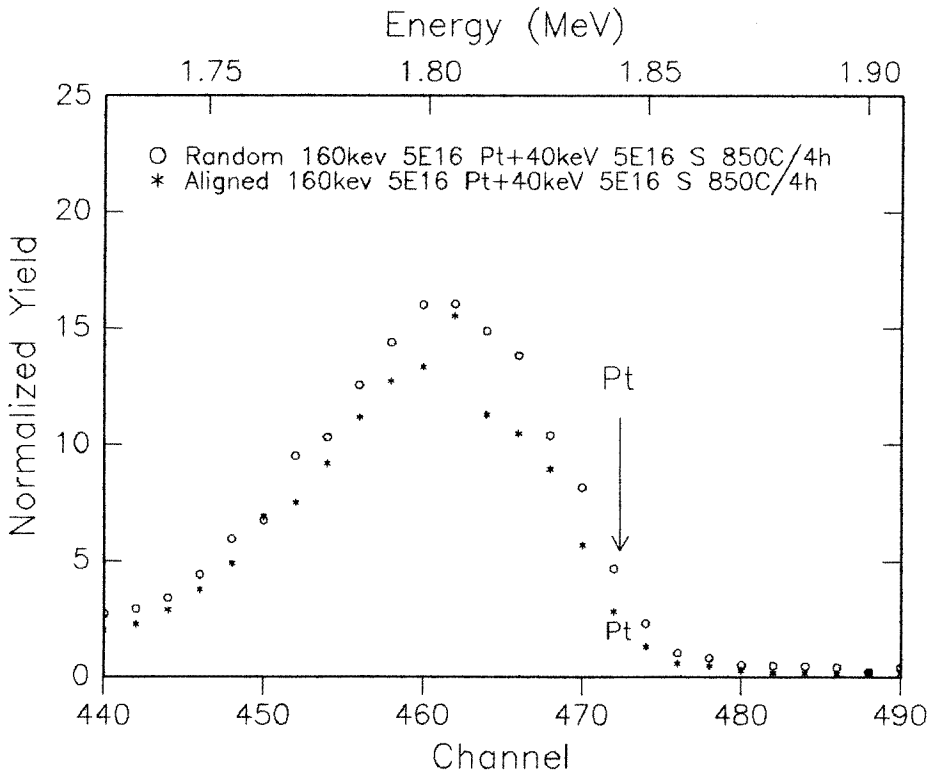

Figure 6. Annealing behaviours of Pt in the 160 keV 5×10^{16} Pt cm^{-2} and 40 keV 5×10^{16} S cm^{-2} implanted sample at 850 °C for 4 hours (the scattering angle is 170°, energy calibration is: $\epsilon = 3.63$ keV/channel and $E_0 = 129.0$ keV).

1100 °C/12 hours annealing in air ambient. XRD measurement confirmed the formation of platinum crystallites (as shown in figure 2) during thermal annealing. These platinum precipitates have ⟨200⟩ preferred orientation, which is consistent with the results (as shown in figure 5) that the aligned Pt spectrum yield is much lower than that of the random spectrum, and with the results of angular scanning about the ⟨100⟩ axial channel of YSZ implanted with 158 keV platinum reported by D X Cao *et al* [15]. Roberts [9] reported that the Pt film vapour-deposited onto a YSZ(100) crystal formed particles after thermal treatment at above 350 K, and the Pt particles were oriented with the hexagonal (111) plane parallel to the ZrO_2(100) surface, even after the formation of very large particles, by transmission electron diffraction (TED) measurement. Consequently, they concluded that Pt interacts strongly with the ZrO_2 substrate at the surface. It can also be seen from figure 2 that for the platinum singly implanted samples a small fraction of the platinum grains has ⟨111⟩ orientation after annealing at 1100 °C, but no precipitates with ⟨11⟩ orientation were observed after annealing at 850 °C by XRD measurement (not shown here). The preferred orientation of platinum grains revealed that the crystallization of implanted platinum was affected by the YSZ matrix. As shown in figure 4, after dual implantation followed by annealing at 850 °C/4 hours, the height of the ⟨111⟩ diffraction peak of Pt crystallites is the same as the ⟨200⟩ diffraction peak, and the ⟨220⟩ and ⟨222⟩ diffraction peaks were also observed, which indicated that the platinum grains were oriented randomly. This XRD

result is consistent with the RBS-C result (shown in figure 6) that the aligned spectrum almost overlaps with the random spectrum of Pt distribution.

Figure 4 also confirms the formation of hexagonal PtS_2 with ⟨111⟩ orientation; the PtS_2 grain size was estimated from the Scherrer formula [16] ($D = 0.9\lambda/\beta \cos\theta$) to be about 4.5 nm. This result reveals that the interaction between sulphur and platinum in YSZ material is relatively strong. The formation of PtS_2 may be one of the factors that affect the lifetime of oxygen sensors. Since particle morphology can change the reactivity for certain reactions by several orders of magnitude [17,18], the existence of sulphur could influence the catalytic properties of Pt for decomposition of oxygen simply by affecting the concentration of different facets, which is under investigation.

4. Conclusion

The results obtained in this work can be summarized as follows.

(1) Single-crystal samples of ⟨100⟩ oriented cubic zirconia stabilized with 9.5 mol% yttria were not amorphized after 160 keV 5×10^{16} Pt cm^{-2} followed by 40 keV 2×10^{16} S cm^{-2} or 5×10^{16} S cm^{-2} implantation.

(2) Recrystallization of the YSZ damage layer formed by 160 keV 5×10^{16} Pt cm^{-2} single implantation induced formation of Pt crystallites with ⟨200⟩ preferred orientation during annealing at 1100 °C.

(3) For dual implantation sulphur enhanced formation of polycrystalline monoclinic zirconia and caused the Pt grains to orientate randomly.

(4) For dual-implanted samples, XRD measurement shows the formation of hexagonal PtS_2 grains with a size of about 4.5 nm after 850 °C/4 hours annealing.

References

[1] Subbarao E C and Maiti H S 1984 *Solid State Ion.* **11** 317
[2] Traversa E 1995 *Sensors Actuators* B **23** 135
[3] Aoki S, Fukutomi M, Komori K and Meada H 1994 *J. Vac. Sci. Technol.* A **12** 501
[4] Li Q, Meyer O, Xi X X, Geerk J and Linker G 1989 *Appl. Phys. Lett.* **55** 1792
[5] Singh R K, Narayan J, Singh A K and Krishnaswamg J 1989 *Appl. Phys. Lett.* **54** 2271
[6] Winnubst A J A, Scharenborg A H A and Burggraaf A J 1984 *Solid State Ion.* **14** 319
[7] Matsui N and Tahigawa M 1990 *Solid State Ion.* **40/41** 926
[8] Neubeck K, Nitsche R, Hahn H, Alberts L, Wolf G K and Friz M 1995 *Nucl. Instrum. Methods* B **106** 926
[9] Roberts S and Gorte R J 1991 *J. Phys. Chem.* **95** 5600
[10] Dilara P A and Vohs J M 1995 *J.Phys.Chem.* **99** 17 259
[11] Olmer L J and Isaacs H S 1982 *J. Electochem. Soc.* **129** 345
[12] Fouletier J, Seinera H and Kleitz M 1974 *J. Appl. Electrochem.* **4** 305
[13] Xie D Z, Zhu D Z and Cao D X *Nncl. Instrum. Methods* B submitted
[14] Xie D Z, Zhu D Z and Cao D X *Nucl. Instrum. Methods* B **122** 55
[15] Cao D X, Sood D K and Brown I G 1994 *Nucl. Instrum. Methods* B **91** 280
[16] Dayal R D, Gokhale N M, Sharma S C, Rams Lal and Krishan R Br 1992 *Ceram. Trans. J.* **91** 45
[17] Lee C, Schmidt L D, Mouldr J F and Rusch T W 1986 *J. Catal.* **99** 472
[18] Lee C and Schmidt L D 1986 *J.Catal.* **101** 123